

Of Winds and Waves

John G. Kirk¹ and Ioanna Arka²

¹Max-Planck-Institut für Kernphysik, Postfach 10 39 80, 69029 Heidelberg, Germany

²Institute de Planetologie et d'Astrophysique, University of Grenoble, Grenoble, France

E-mail: john.kirk@mpi-hd.mpg.de

Abstract. Recent work on the properties of superluminal waves in pulsar winds is summarized. It is speculated that these waves play an important role in the termination shock that divides the wind from the surrounding nebula.

1. Introduction

In addition to pulses of radiation, rotation-powered pulsars are thought to emit a wind that powers the diffuse radiation or *pulsar wind nebulae* (PWN) observed around many of them in the radio, optical, X-ray and gamma-ray bands. Synchrotron emission and inverse Compton scattering are the mechanisms most likely to be at work in PWN, and it has been evident for over half a century that not only the energy, but also both the relativistic electrons (or positrons) and the magnetic fields in these nebulae must be supplied by the central star[1].

The basic idea is that the rotation of the neutron star couples to the wind through the strong magnetic field anchored in its crust [2, 3]. As well as electromagnetic fields oscillating at the rotation frequency of the pulsar, the wind contains a DC (phase-averaged) component of the magnetic field, electrons and positrons created by cascades in the magnetosphere and, perhaps, a relatively small number of electrons and ions extracted from the stellar surface. As it propagates away from the star, the ram pressure of the wind decreases, and, roughly where it equals the ambient pressure, a *termination shock* is formed. Rees & Gunn [3] simply assumed that the waves are absorbed at the termination shock, leaving behind the energized particles and magnetic fields that fill the nebula. Kundt & Krotscheck [4], however, noted that electromagnetic waves could also be reflected by the shock and build up inside it. This raises an important question concerning the structure of the termination shock and the wind it encloses. Because the waves have large amplitude, they interact strongly with each other and with the particle component. Rather than just a linear superposition of DC fields, particles, outward propagating waves and reflected waves, one must, therefore, look for self-consistent solutions, containing all of these, that match the outer boundary conditions.

2. The σ problem

Estimates of the energy density in magnetic field at the light cylinder $r_L = c/\omega$ (with ω the angular frequency of the pulsar) suggest that the wind is energetically

dominated at launch by the waves and/or DC fields. On the other hand, outside the termination shock the particle pressure is comparable or larger than the pressure exerted by the fields (for reviews, see [5, 6]). The implied conversion of electromagnetic into kinetic energy is quite natural in many situations, for example, when an MHD outflow is collimated and accelerated into a jet. However, this kind of conversion does not appear possible in a pulsar wind, where the poloidal flux threads the neutron star [6]. In such a case, the MHD equations suggest the flow remains radial and its (supermagnetosonic) speed stays constant until the termination shock is reached.

This, then, is the “ σ problem” (the ratio of Poynting to kinetic energy flux is conventionally denoted by σ): if the pulsar wind can be described by the equations of ideal MHD, there is no way in which a large value of σ near the star can be reduced to unity or below before the termination shock is reached. Furthermore, if the termination shock is simply a discontinuity that obeys the usual jump conditions in an otherwise ideal MHD flow, the downstream plasma remains magnetically dominated with large σ .

3. Dissipation in current sheets

To solve this problem, we obviously need to go beyond the ideal MHD description [7]. One possibility, suggested by Coroniti [8] and Michel [9], is to allow for dissipation in a current sheet embedded in a wind that is otherwise a cold, MHD flow. This is the “striped wind” picture. Conversion of the energy flux from fields to particles by dissipation in the sheets causes the flow to accelerate [10, 11, 12] — in the simplest model the bulk Lorentz factor rises as $\Gamma \propto r^{1/2}$. Consequently, time-dilation reduces the effective dissipation rate seen in the lab. frame. It is possible to place upper and lower limits on the dissipation rate in order to constrain the characteristic radius at which the oscillating components of the fields are annihilated. The results depend on the pair-loading of the flow, described by the parameter

$$\mu = \frac{L}{\dot{M}c^2} \quad (1)$$

where L is the luminosity and \dot{M} the mass-loss rate. For the Crab, dissipation occurs before the termination shock is reached only if $\mu < 10^4$, a value somewhat lower than conventional estimates [13].

Embedded current sheets also change our picture of the termination shock. On the basis of an analytical model and 1D PIC simulations, Lyubarsky & Liverts [14] and Pétri & Lyubarsky [15] suggested that an MHD shock sweeping through the cold portions of the striped wind would drive reconnection in the embedded current sheets and dissipate a substantial fraction of the magnetic energy, provided the resulting heated electrons were unmagnetized. For $\sigma \gg 1$, this is equivalent to the condition

$$\mu > a \quad (2)$$

where the strength parameter a of the incoming wave (striped wind) is the ratio of the quiver frequency of the electrons eB/mc to the angular frequency ω of the

wave. (see [16]).¹ Since a decreases as $1/r$ in spherical geometry, (2) amounts to a lower limit on the radius at which such a process could operate:

$$\begin{aligned} r &> r_{\text{crit}} \\ &\approx 3.4 \times 10^{10} r_{\text{L}} L_{38}^{1/2} / \mu \end{aligned} \quad (3)$$

where $(L_{38}/4\pi) \times 10^{38}$ erg/s is the luminosity per unit solid angle carried by the wind.

On the other hand, Sironi & Spitkovsky [18] recently considered driven reconnection in the striped wind using 2D and 3D PIC simulations. Although their investigations were confined to the range $0.05 < r/r_{\text{crit}} < 4$, they found substantial dissipation in all cases. They also noted the appearance of high-energy particles accelerated by the first-order Fermi mechanism, and, on the basis of a comparison of the nonthermal particle spectrum with the observed synchrotron spectrum, suggested that, in the case of the Crab, the termination shock should be located where $r \approx r_{\text{crit}}/3$. If this interpretation is correct, the radius of the termination shock inferred from X-ray observations (~ 0.1 pc) implies $\mu \sim 50$. This is much smaller than conventionally estimated, implying a very high pair loading and a mildly relativistic $\Gamma \sim 10$ outflow. An approximately spherically symmetric wind with these parameters would vastly overpopulate the nebula with electrons and positrons. However, if we interpret the wind parameters and, therefore, the radius of the termination shock, as latitude dependent, it cannot be ruled out that some part of the wind, for example the equatorial plane, contains a relatively dense, slow outflow of the type suggested.

4. Charge starvation

As well as giving rise to dissipation in current sheets, non (ideal-)MHD effects can also manifest themselves via charge starvation, which can arise, for example, when the required currents demand relativistic motion of the current carriers [19, 20]. A relativistic two-fluid (electron-positron) approach can be used to model this effect. In the simplest case, with cold fluids and charge neutrality, both subluminal and superluminal nonlinear waves can be found [16].

The subluminal wave resembles the striped wind, except that the current sheet is replaced by a static shear, with $|\vec{B}|^2$ constant (i.e., a circularly polarized wave). The phase profile of the shear can be chosen arbitrarily, but it is monochromatic in the simplest case of constant density. It is interesting to note that, as for the striped wind, the non-MHD effects cause also this solution to accelerate with radius, in this case with $\Gamma \propto r$, despite the fact that no dissipation process is involved [19]. However, at least for the monochromatic wave, acceleration starts relatively far from the pulsar, where

$$\sigma > a \quad (4)$$

¹ There are several ways to define this important parameter. In the striped wind, where $|B|$ is phase-independent and $\sigma \gg 1$, there is no ambiguity. For the superluminal waves discussed in section 5 we take $a = eE_{\text{max}}/mc\omega$, where E_{max} is the amplitude of the oscillating electric field. A covariant, gauge-independent definition for vacuum waves is given by Heinzl & Ilderton [17]

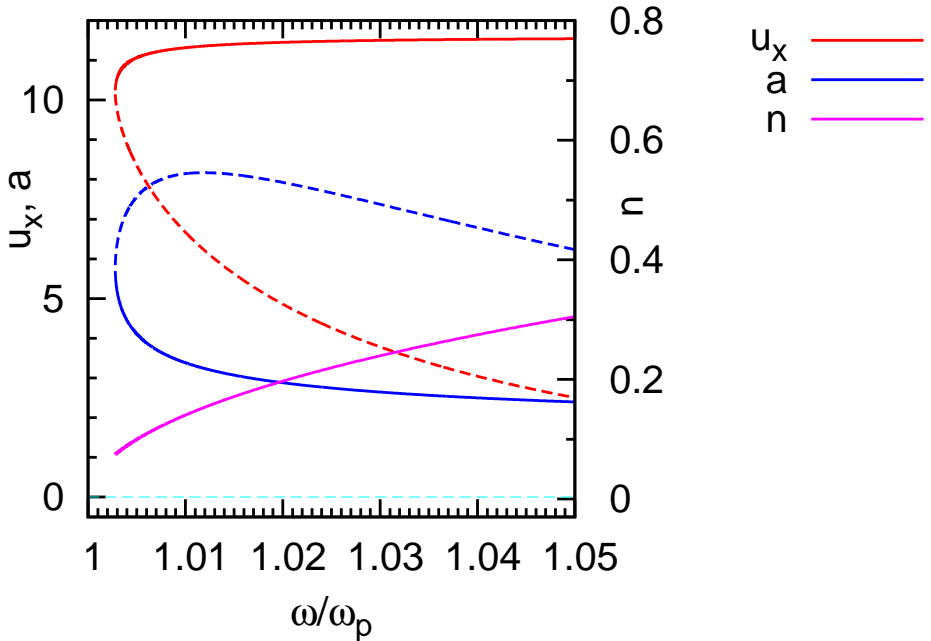


Figure 1. The radial four-velocity of the fluid, the strength parameter a , and the refractive index n of circularly polarized superluminal waves close to the cut-off frequency for $\mu = 12$, $\sigma = 3$.

corresponding to

$$r > \Gamma r_{\text{crit}} \quad (5)$$

The solutions with superluminal phase speed resemble vacuum electromagnetic waves, in the sense that the displacement current plays a crucial role. The fields are transverse, and satisfy $|\vec{E}| > |\vec{B}|$. The waves and particles are not locked together in the way they are in the subluminal solutions, which makes them more promising candidates for matching to a boundary condition at the termination shock. There have been extensive investigations of these waves in the literature (see [21] and references therein). They propagate only when the density falls below a critical value. In spherical geometry, the corresponding condition on the radius coincides with (3). Because of this, they cannot be launched close to the pulsar, and can only be realized if a striped-wind-like (subluminal) solution converts into a superluminal one either spontaneously, or because it is forced to do so by the boundary condition imposed by the termination shock. In this case, the conversion process and subsequent radial evolution and damping of the mode should more properly be regarded as an integral part of the “termination shock” structure.

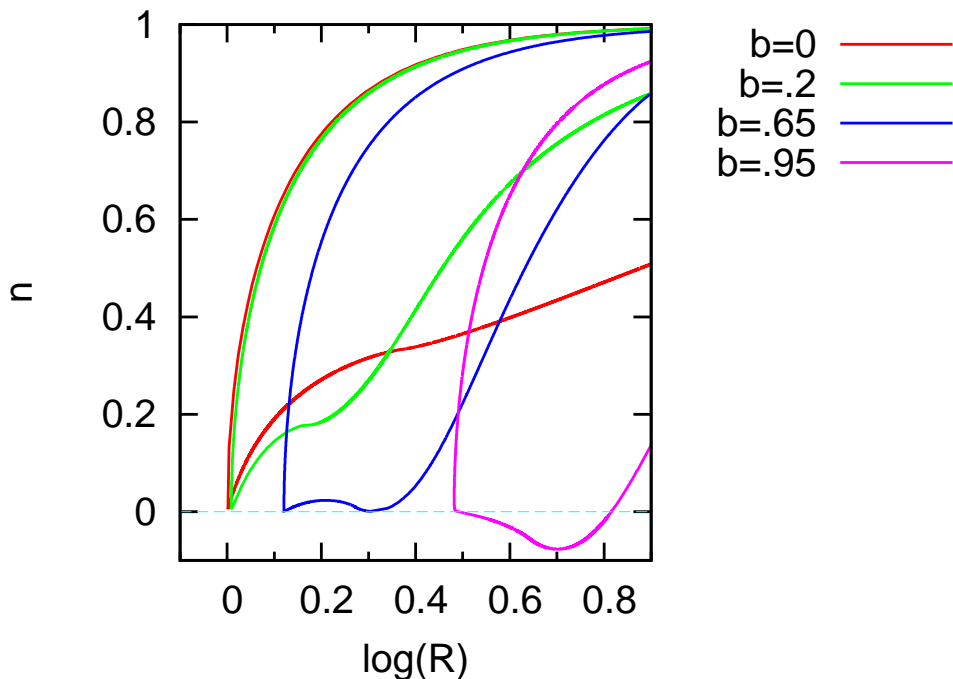


Figure 2. The refractive indices of linearly polarized superluminal waves close to the cut-off frequency for $\mu = 10100$, $\sigma = 100$ as a function of radius normalized to r_{crit} (see Eq. 3), for different values of the phase-averaged magnetic field

5. Superluminal waves

A first step towards understanding the role of superluminal waves is to determine the propagation characteristics of those waves to which a given striped (or other subluminal) wind can convert. This amounts to solving the two-fluid analogue of the shock jump conditions. Here we present a brief summary of some recent work on this topic — a full description can be found in [21].

Circularly polarized modes with zero phase-averaged field are the simplest to analyze, since the jump conditions can be solved analytically [16]. Figure 1 illustrates the properties of these waves for parameters $\mu = 12$, $\sigma = 3$ (and, therefore, $\Gamma = 3$). Although not in the range expected in pulsar winds, this parameter set reveals the mode structure near the cut-off frequency particularly clearly. The figure shows that for each value of the frequency ω in the lab. frame, measured in units of the proper plasma frequency ω_p , two solutions exist that carry the prescribed particle, energy and momentum fluxes: a strong wave through which the plasma streams relatively slowly (dashed line) and a weaker one (solid line) through which the plasma streams rapidly (u_x is the four velocity along the propagation direction). Transition to the the weak wave involves almost complete annihilation of the incoming field energy, leading to $u_x \approx \mu$. The refractive indices of these modes coincide and correspond to superluminal phase speed $n < 1$. Because of the finite wave amplitude, the lab. frame frequency ω exceeds the proper plasma frequency ω_p , which equals the cut-off frequency for linear waves.

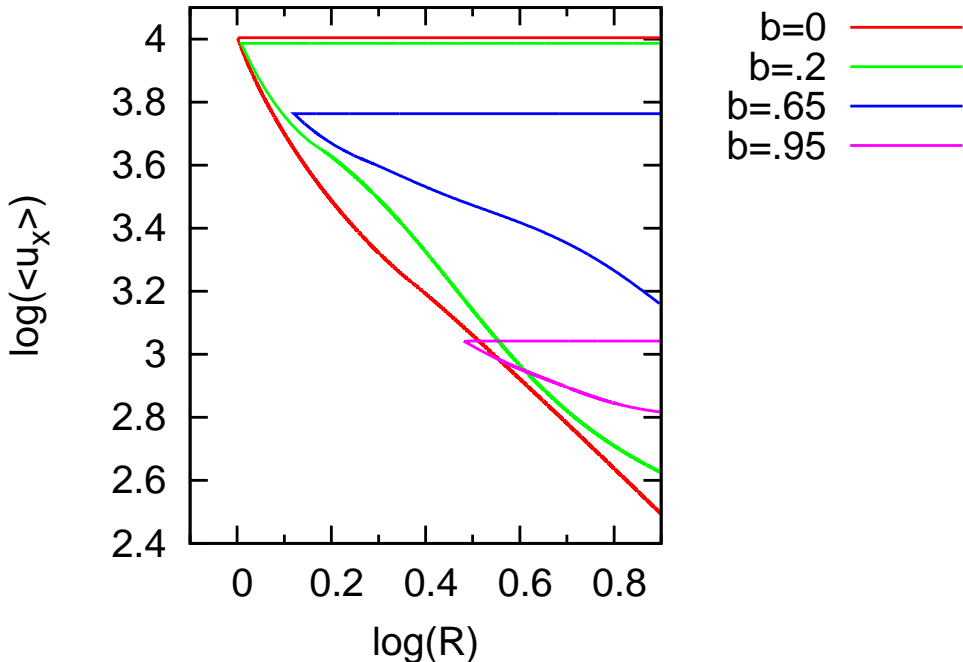


Figure 3. The phase-averaged radial four-speed of the electron and positron fluids in the linearly polarized superluminal waves shown in Fig. 2.

Linearly polarized waves are much more complicated, requiring a numerical solution to the jump conditions. Nevertheless, the properties illustrated in Fig. 1 apply also to these modes. Two solutions are available for each set of “upstream” parameters that characterize the corresponding subluminal solution. This is shown in Fig. 2, which differs from Fig. 1 in two ways. Firstly, we show the refractive index not as a function of frequency, but of radius in the pulsar wind, normalized to r_{crit} given in Eq. (3). In this representation, the refractive indices of the two solutions no longer coincide, since the proper plasma frequencies associated with each solution, differ although the lab. frame densities do not. Secondly, we show solutions for four different values of the phase-averaged magnetic field, given by the parameter $b = \langle \vec{B} \rangle / \langle B^2 \rangle^{1/2}$. It can be seen that stronger DC fields push the cut-off radius further out from the pulsar. Furthermore, stronger fields display solutions with negative refractive index, corresponding to phase velocities directed radially inwards. Figure 3 shows the phase-averaged four-velocity of the plasma stream in the radial direction. Note that the weak wave has $\langle u_x \rangle \approx \mu$ only for zero averaged field. For finite values of the DC field, only a fraction of the incoming Poynting flux is carried by the oscillating fields and can be annihilated.

6. Summary

Because they are powerful enough to evacuate a relatively large cavity, pulsar winds provide an environment in which electromagnetic fields dominate the

dynamics, and, especially in the outer regions, non-MHD effects are crucial. Within the critical radius given by (3), energized electrons and positrons, which have Lorentz factors $\sim \mu$, can be regarded as magnetized, since their relativistic Larmor radius, $\mu mc^2/eB$ (which in this case equals the effective inertial length c/ω_p) is smaller than the length scale c/ω . Here the superluminal modes cannot propagate, because the plasma is sufficiently dense to screen out electromagnetic waves reflected from the termination shock. In this region, 2D and 3D PIC simulations indicate that dissipation could be driven by a standing shock front [18]. However, in the case of isolated pulsars, r_{crit} lies well inside the point of pressure balance with the external medium, making it doubtful that such a shock could be supported.

Outside r_{crit} energized particles are unmagnetized. Driven reconnection at the termination shock may still occur [15], but superluminal waves may also play an important role. In section 5 we have briefly summarized some recent work [21] on the properties of these waves for parameters thought appropriate in pulsar winds, and sketched their possible role. Although the physics of these two scenarios remains to be investigated in detail, it seems likely that there will be observable implications. Indeed, current sheets have been proposed as the source of both the pulsed high-energy emission [22, 23] as well as the recently observed flares in very high energy gamma-rays from the Crab [24, 25].

References

- [1] Piddington J H 1957 *Australian Journal of Physics* **10** 530–+
- [2] Pacini F 1967 *Nature* **216** 567–+
- [3] Rees M J and Gunn J E 1974 *MNRAS* **167** 1–12
- [4] Kundt W and Krotscheck E 1980 *A & A* **83** 1–21
- [5] Gaensler B M and Slane P O 2006 *Ann. Rev. Astron. Astrophys* **44** 17–47 (*Preprint arXiv:astro-ph/0601081*)
- [6] Kirk J G, Lyubarsky Y and Petri J 2009 *The Theory of Pulsar Winds and Nebulae Astrophysics and Space Science Library (Astrophysics and Space Science Library vol 357)* ed W Becker pp 421–+
- [7] Lyutikov M 2010 *MNRAS* 581–+ (*Preprint 0911.0324*)
- [8] Coroniti F V 1990 *Astrophys. J.* **349** 538–545
- [9] Michel F C 1994 *Astrophys. J.* **431** 397–401
- [10] Lyubarsky Y and Kirk J G 2001 *Astrophys. J.* **547** 437–448 (*Preprint arXiv:astro-ph/0009270*)
- [11] Drenkhahn G 2002 *A & A* **387** 714–724 (*Preprint arXiv:astro-ph/0112509*)
- [12] Lyubarsky Y 2010 *Astrophys. J. Lett.* **725** L234–L238 (*Preprint 1012.1411*)
- [13] Kirk J G and Skjæraasen O 2003 *Astrophys. J.* **591** 366–379 (*Preprint arXiv:astro-ph/0303194*)
- [14] Lyubarsky Y and Liverts M 2008 *Astrophys. J.* **682** 1436–1442 (*Preprint 0805.0085*)
- [15] Pétri J and Lyubarsky Y 2007 *A & A* **473** 683–700
- [16] Kirk J G 2010 *Plasma Physics and Controlled Fusion* **52** 124029–+ (*Preprint 1008.0536*)
- [17] Heinzl T and Ilderton A 2009 *Optics Communications* **282** 1879–1883 (*Preprint 0807.1841*)
- [18] Sironi L and Spitkovsky A 2011 *ArXiv e-prints (Preprint 1107.0977)*
- [19] Kirk J G and Mochol I 2011 *Astrophys. J.* **729** 104–+ (*Preprint 1012.0307*)
- [20] Kirk J G and Mochol I 2011 *Astrophys. J.* **736** 165–+
- [21] Arka I and Kirk J G 2011 *ArXiv e-prints (Preprint 1109.2756)*
- [22] Pétri J 2011 *MNRAS* **412** 1870–1880 (*Preprint 1011.3431*)
- [23] Pétri J and Dubus G 2011 *MNRAS* 1193–+ (*Preprint 1104.4219*)
- [24] Uzdensky D A, Cerutti B and Begelman M C 2011 *Astrophys. J. Lett.* **737** L40+ (*Preprint 1105.0942*)

[25] Cerutti B, Uzdensky D A and Begelman M C 2011 *ArXiv e-prints* (*Preprint 1110.0557*)